

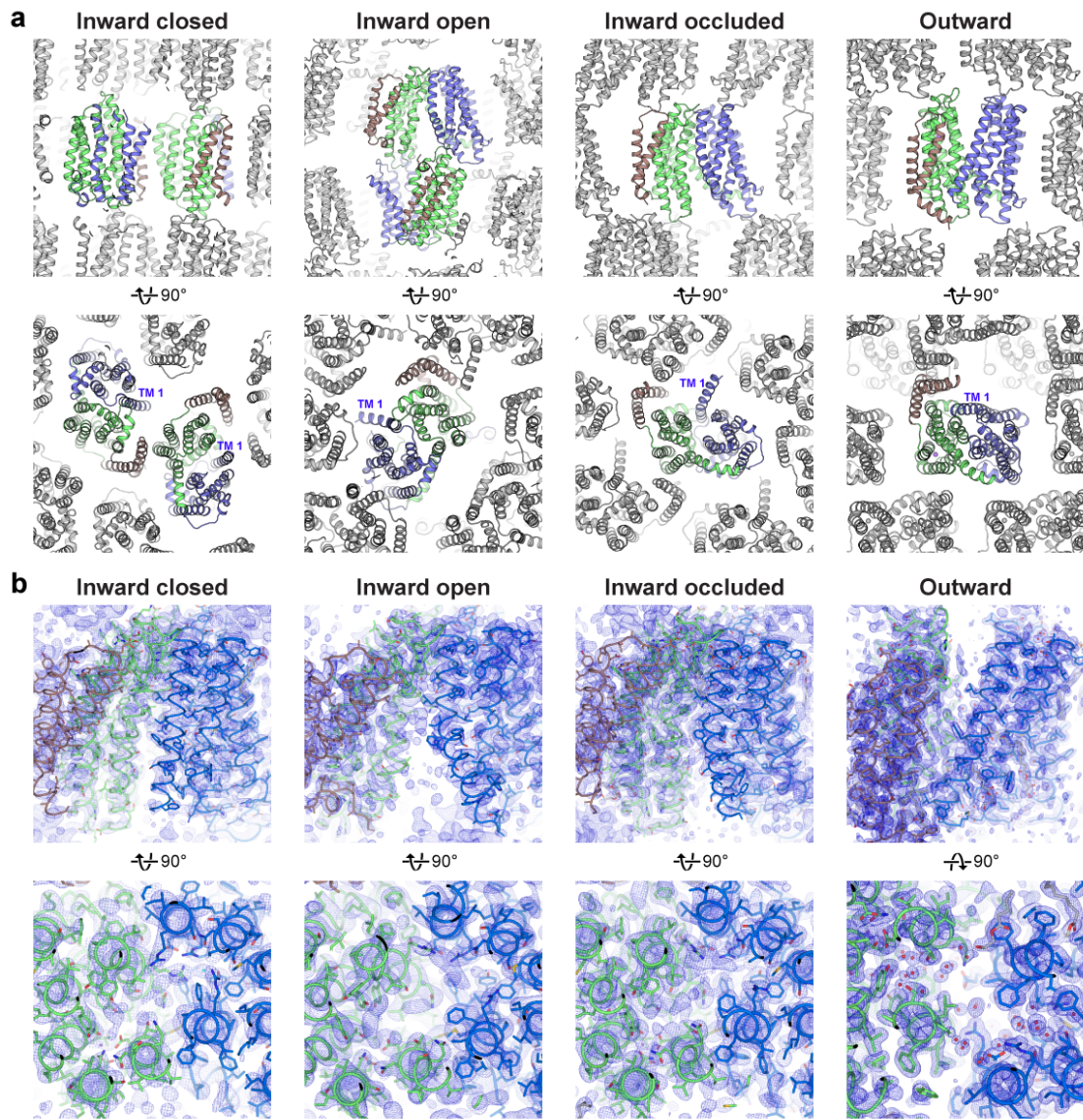
Supplementary Information

Visualizing Conformation Transitions of the Lipid II Flippase MurJ

Kuk et al.

12 Supplementary figures

4 Supplementary tables



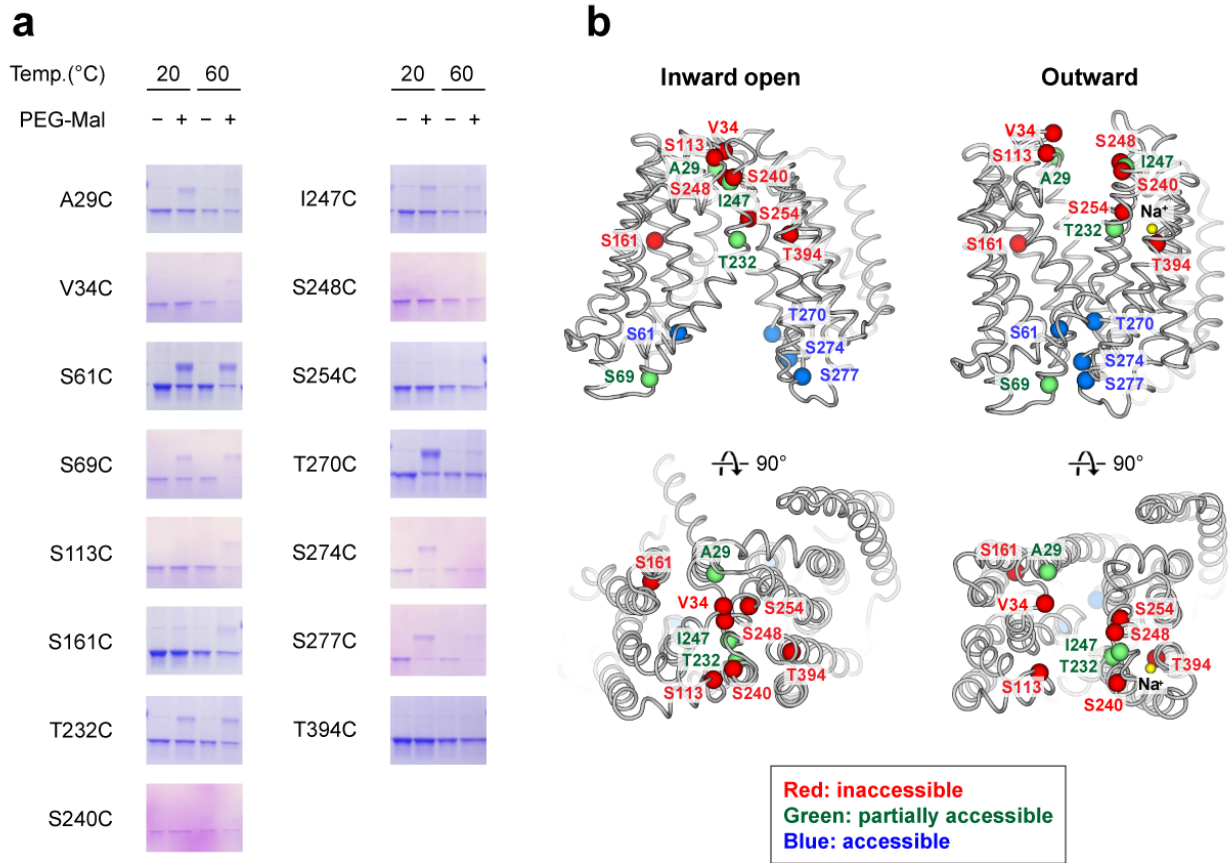
Supplementary Figure 1. Crystal packing and electron density in the MurJ_{TA} structures. a.

Crystals were obtained in lipidic cubic phase doped with Lipid II. Crystal contacts are mostly formed by end-to-end stacking, as well as lateral interactions mediated by the host lipid monoolein. TM 1 was not involved in crystal packing and thus its bending is unlikely to be a crystallographic artifact. The asymmetric unit is colored, while symmetry mates are shown in gray.

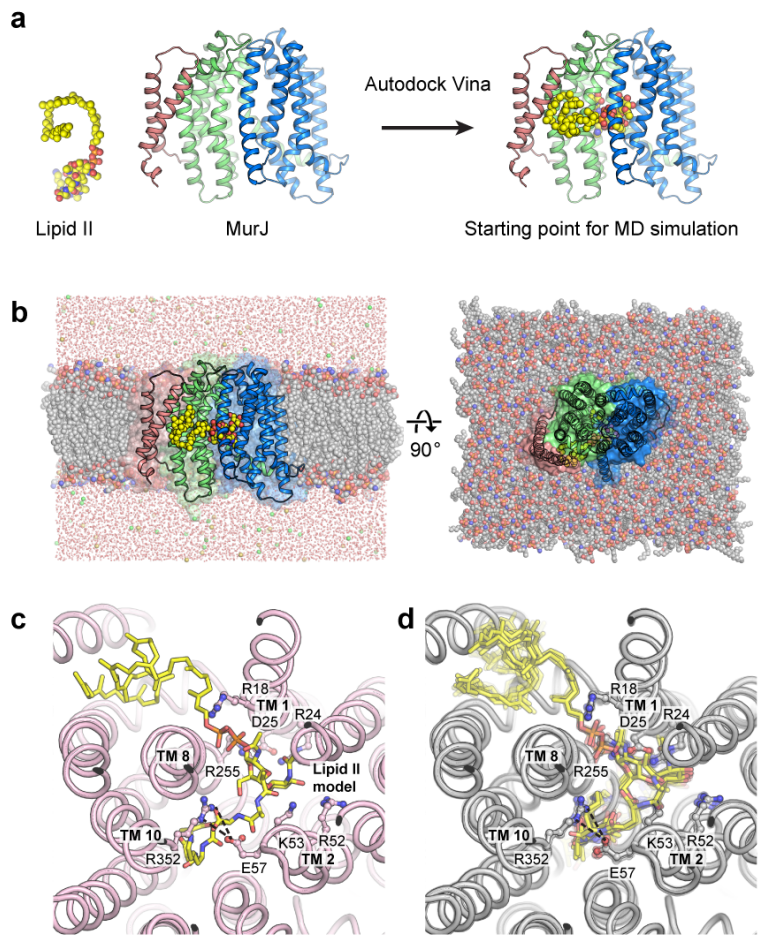
b. 2Fo – Fc composite omit electron density maps (contoured to 1 σ), omitting 5% of the model at a time. Resolutions are (from left) 3.2 Å, 3.0 Å, 2.6 Å, and 1.8 Å.

Supplementary Figure 2. Alignment of MurJ sequences. Positions shaded in red are identical in >90% of Gram-negative MurJ sequences in an alignment with 36 sequences, while those shaded gray are similar in >70% of the sequences. Asterisks (*) denote essential residues in MurJ_{TA} of which alanine mutants fail to complement *E. coli* MurJ, as determined previously²⁵. Carets (^) denote residues participating in Na⁺ coordination. Bullets (•) denote other residues discussed in this manuscript. MurJ_{TA} from *Thermosipho africanus* (UniProt ID: B7IE18) was aligned with 36 Gram-negative MurJ sequences from the UniRef50 library (no sequence is more than 50% identical to another). Drug exporters PfMATE and NorM-NG were also included in the alignment for contrast.

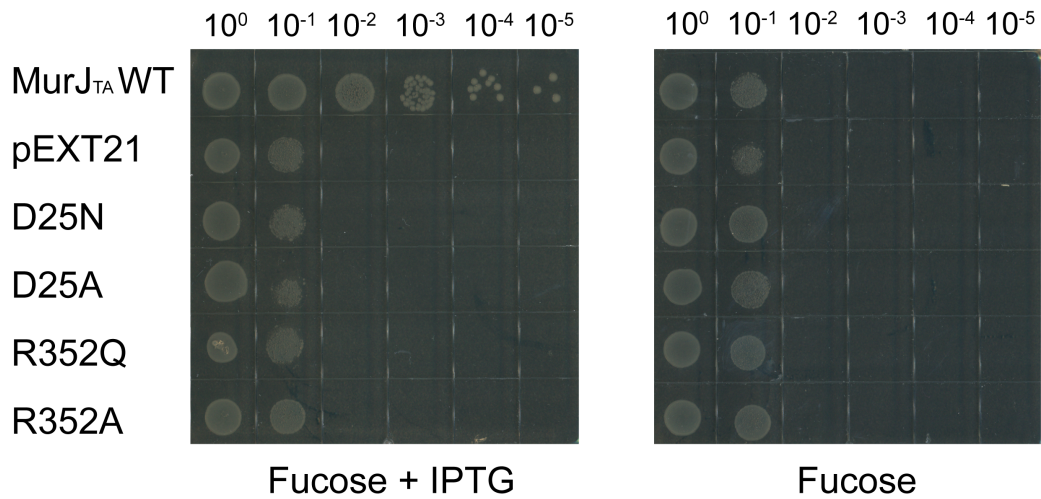
List of sequences shown: MurJ-TA, *Thermosipho africanus* (UniProt ID: B7IE18); MurJ-EC, *Escherichia coli* (P0AF16); MurJ-PF, *Pseudomonas fluorescens* (G8PWV6); MurJ-VC, *Vibrio cholerae* (O34238); MurJ-LI, *Leptospira interrogans* (A0A0C5X9A5); MurJ-RS, *Rhodobacter sphaeroides* (Q3J5H7); PfMATE (PDB ID: 3VVN); NorM-NG (4HUK).



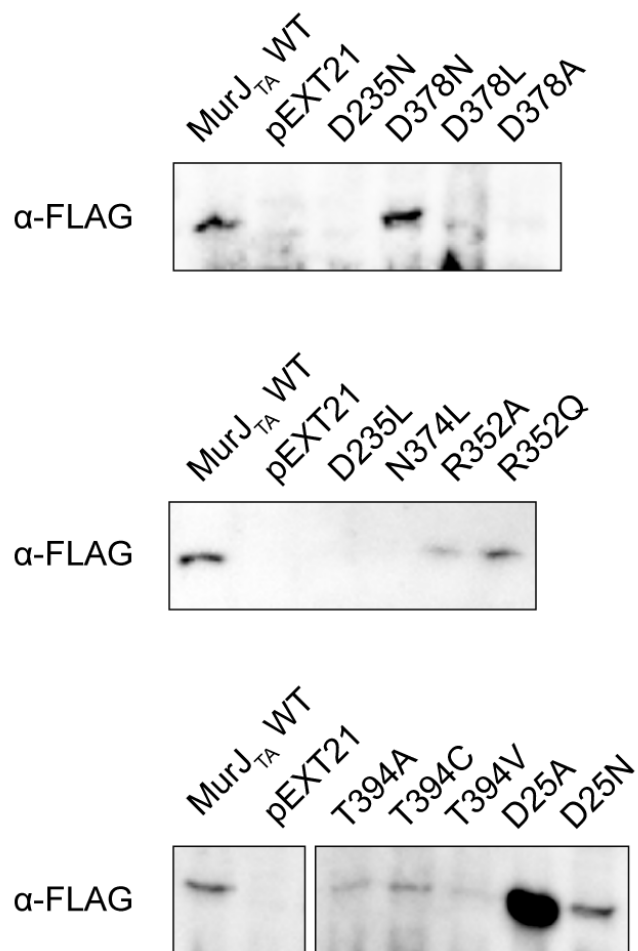
Supplementary Figure 3. MurJ_{TA} assumes a predominantly inward-facing conformation in DDM micelles. **a**, Single cysteine mutants of MurJ_{TA} (no endogenous cysteines) were expressed, purified, delipidated, and probed for accessibility in DDM micelles by a direct labeling strategy in potassium acetate (absence of sodium). Accessible cysteines would be labeled by PEG5000-maleimide (PEG-Mal), resulting in a mass shift up the gel. Experiments were performed at either 20°C or 60°C. Source data are provided as a Source Data File. **b**, Mapping of these cysteine positions (for the 20°C data) to the inward-open and outward-facing crystal structures of MurJ_{TA}. Positions were considered inaccessible if only the lower band was observed, and accessible if the top band was observed and of higher intensity than the lower band. Remaining positions with both bands visible were considered partially accessible.



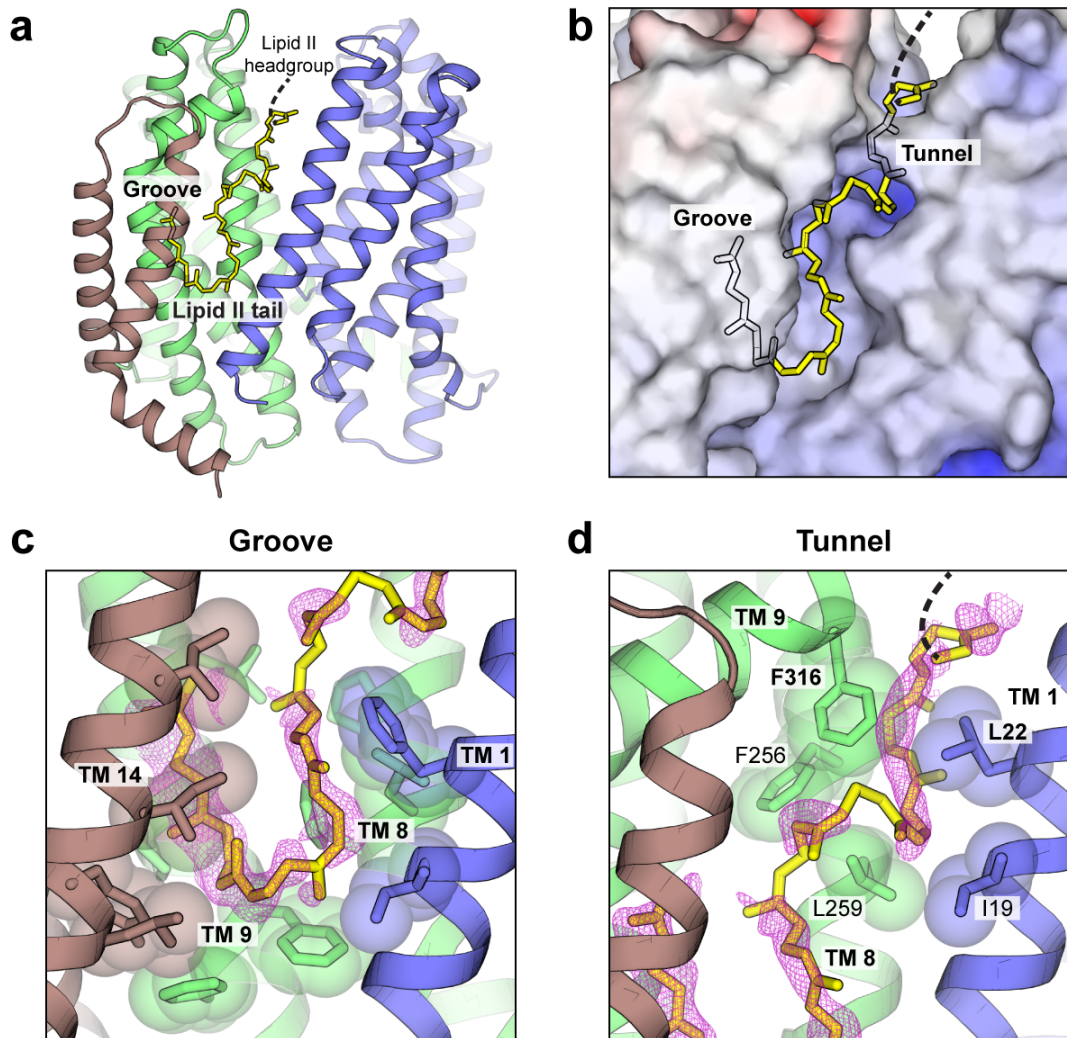
Supplementary Figure 4. Docking and MD simulation of Lipid II to the inward-occluded structure. **a**, Lipid II (yellow spheres) was docked to the inward-occluded structure by Autodock Vina. **b**, The docking result was used as a starting point for molecular dynamics simulation by NAMD in a hydrated and ionized (150 mM NaCl) POPE membrane bilayer system. The equilibrated system is shown, with lipids visualized as spheres and waters denoted by red dots. **c**, Cytoplasmic view of the docked complex (Lipid II shown as yellow sticks, charged residues in the cavity shown as gray sticks), showing how the Glu57-Arg352 thin gate could help occlude the substrate. **d**, Rotation of MurJ sidechain and Lipid II torsions in a molecular dynamics simulation starting from the docked model, visualizing the picosecond dynamics of the docked MurJ-Lipid II complex (snapshots at each 10 ps overlaid, total 100 ps). Surrounding lipids and waters are hidden for clarity.



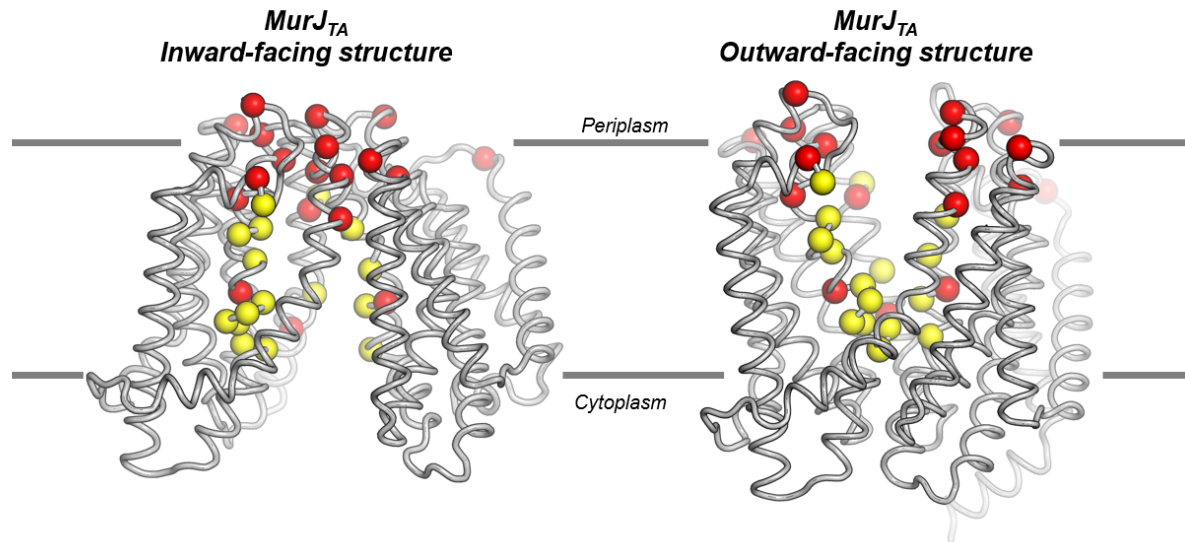
Supplementary Figure 5. Complementation assay of MurJ_{TA} Asp25 and Arg352 mutants in *E. coli* NR1154. Cells transformed with plasmids encoding MurJ_{TA} (wild-type or mutant) or without insert (pEXT21) were depleted of endogenous *E. coli* MurJ by serial dilution on plates containing the anti-inducer D-fucose. MurJ_{TA} expression was induced by addition of IPTG. Data shown are representative of three biological replicates. Source data are provided as a Source Data File.



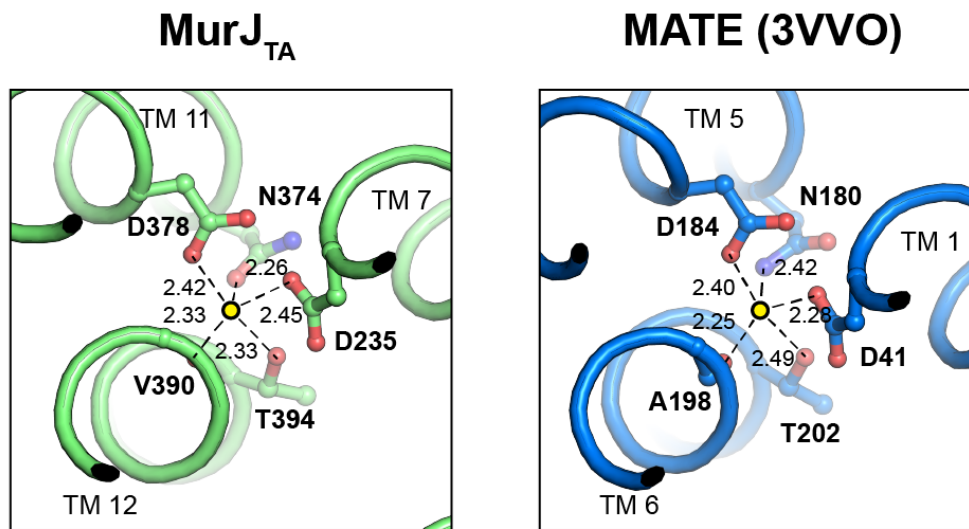
Supplementary Figure 6. Western blot analysis of MurJ_{TA} mutants. MurJ_{TA} proteins carrying a C-terminal FLAG tag were expressed by the addition of 0.1 mM IPTG in the presence of arabinose. Total membrane fractions were isolated by ultracentrifugation and probed by mouse anti-FLAG primary antibody and horseradish peroxidase-conjugated anti-mouse secondary antibody. Source data are provided as a Source Data File.



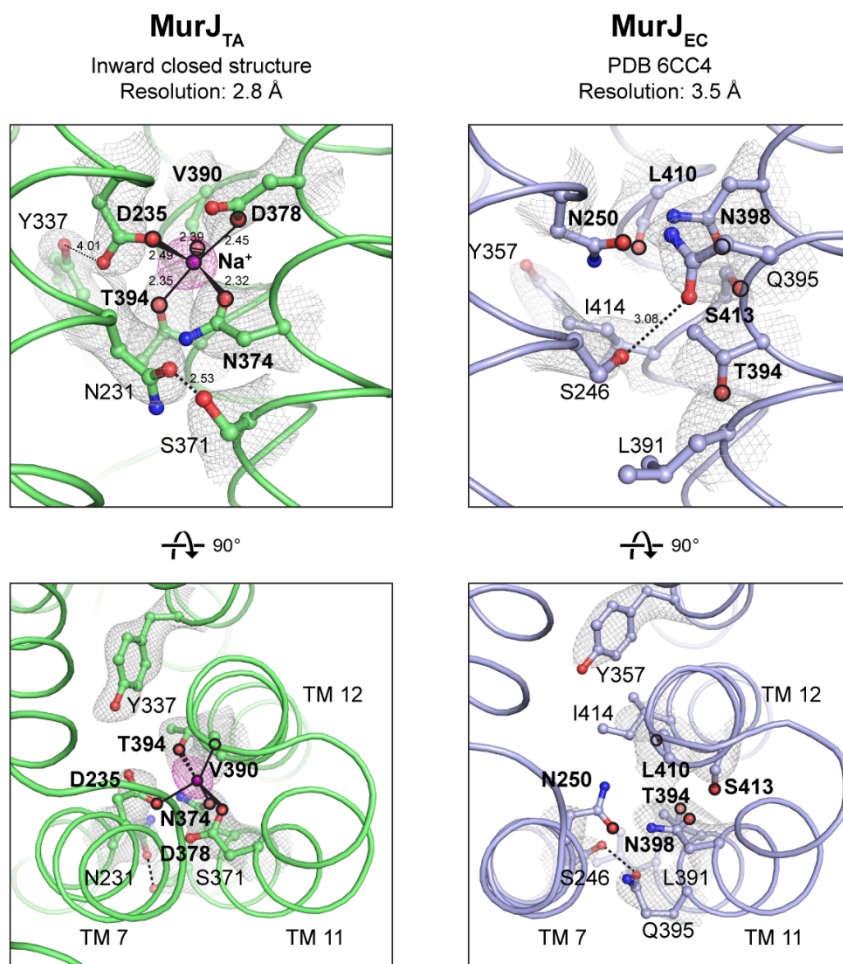
Supplementary Figure 7. Structural features of the putative lipid-binding site in the outward state. **a**, Putative lipid-binding site. Yellow sticks denote a model of the undecaprenyl tail of Lipid II, which was never used for structure refinement or map calculation. **b**, The lipid is restrained by the hydrophobic groove and a short tunnel near the periplasmic side. **c-d**, Unmodeled $2F_o - F_c$ electron density peaks (purple mesh, contoured to 0.7σ) were observed in the hydrophobic groove (c), or in the tunnel (d) which is formed by hydrophobic residues Ile19, Leu22, Phe256, Leu259, and Phe316.



Supplementary Figure 8. Mapping of MurJ_{EC} cysteine accessibility data (Butler *et al*, 2013) to MurJ_{TA} structures. Positions accessible to the membrane impermeant reagent MTSES are shown as red spheres, while positions that are partially accessible are shown as yellow spheres. The structures of MurJ_{TA} are consistent with the cysteine accessibility data suggesting a central cavity that is accessible to the periplasm (in the outward-facing conformation).

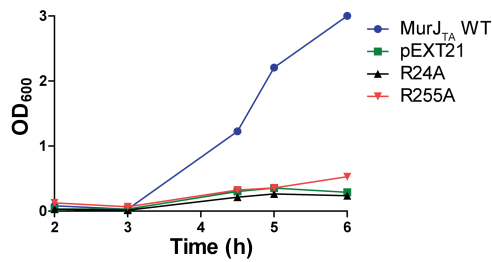


Supplementary Figure 9. The Na⁺ site of MurJ_{TA} is conserved with that of Na⁺ coupled MATE transporters in the same superfamily. MurJ_{TA} is shown on the left, while *Pyrococcus furiosus* MATE (PfMATE) is shown on the right (PDB ID: 3VVO, Tanaka *et al.*, 2013; Ficici *et al.*, 2018), both with a DNDXT composition where X is a backbone carbonyl oxygen.

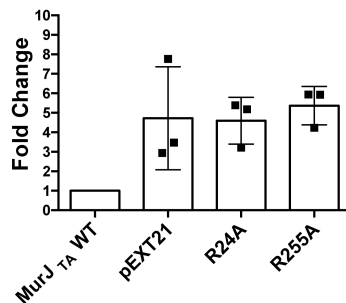


Supplementary Figure 10. The Na⁺ site of MurJ_{TA} is similar with that of MurJ_{EC}. MurJ_{TA} is shown on the left, while MurJ_{EC} is shown on the right (PDB ID: 6CC4, Zheng *et al.*, 2017). The putative sodium-coordinating oxygen atoms (black circles) are conserved.

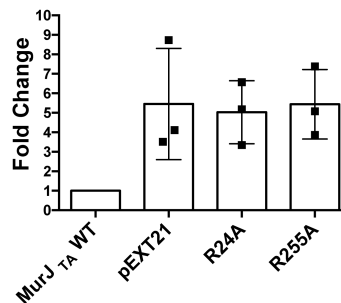
a MurJ Complementation Growth Curve



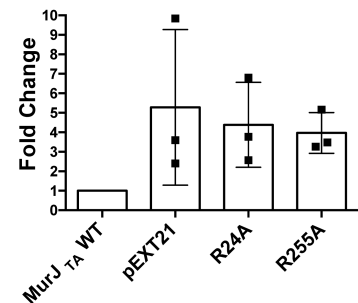
b Lipid II Accumulation (Normalization to Lipid X)



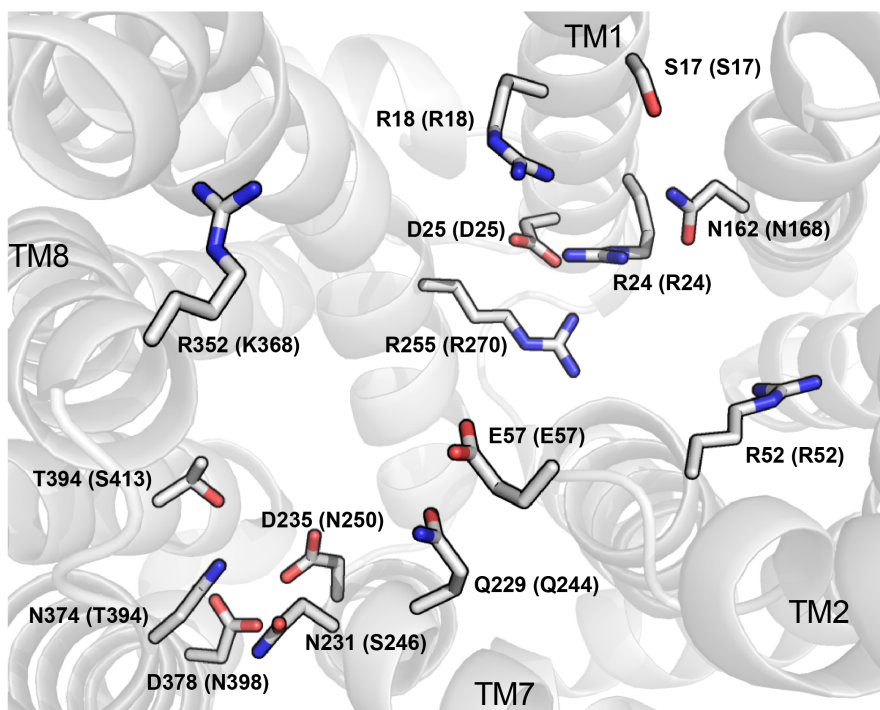
Lipid II Accumulation (Normalization to PE)



Lipid II Accumulation (Normalization to OD₆₀₀)



Supplementary Figure 11. Mass spectrometry assay of cellular Lipid II accumulation. a, Growth curve of *E. coli* MurJ-depletion strain NR1154 expressing MurJ_{TA} wild-type (WT), mutants (R24A/R255A), or empty vector (pEXT21). Cultures were supplemented with D-fucose to deplete endogenous *E. coli* MurJ. At 3 hours post-inoculation, MurJ_{TA} expression was induced with IPTG, and growth was monitored by optical density (OD₆₀₀). **b,** At 6 hours post-inoculation, cells were harvested and cellular Lipid II levels were analyzed by mass spectrometry. Cellular Lipid II levels were normalized against either Lipid X, phosphatidylethanolamine (PE), or cell density (OD₆₀₀). Lipid X is an intermediate in lipopolysaccharide biosynthesis pathway that is separate from the peptidoglycan synthesis pathway, but has similar chemical properties as Lipid II. Normalized Lipid II level of each replicate was divided by that of the wild-type to obtain the fold change. Data are mean \pm s.d., n=3 biological replicates. Source data are provided as a Source Data File.



Supplementary Figure 12. Charged and polar residues in the central cavity of MurJ_{TA} that were subjected to mutagenesis studies. Equivalent position in *E.coli* is in listed in parenthesis.

Supplementary Table 1. Data collection and refinement statistics (molecular replacement)

	Inward closed^a (6NC6)	Inward open^b (6NC7)	Inward occluded^c (6NC8)	Outward^d (6NC9)
Data collection				
Space group	P 2 2 2 ₁	C 2	P 2 2 ₁ 2 ₁	C 2
Cell dimensions				
a, b, c (Å)	71.1, 101.8, 158.5	129.7, 105.5, 111.5	68.4, 80.3, 100.7	128.6, 57.4, 86.4
α, β, γ (°)	90, 90, 90	90, 125.3, 90	90, 90, 90	90, 100.7, 90
Resolution (Å)	85.6–3.2 (3.3–3.2) ^e	74.7–3.0 (3.1–3.0) ^e	68.4–2.6 (2.7–2.6) ^e	84.9–1.8 (1.9–1.8) ^e
<i>R</i> _{pim}	0.15 (0.94)	0.10 (0.83)	0.11 (>1.0)	0.076 (0.71)
<i>I</i> /σ(<i>I</i>)	9.48 (1.14)	11.41 (1.00)	13.29 (1.13)	22.71 (1.09)
Completeness (%)	99.4 (99.3)	99.0 (98.0)	99.8 (99.7)	99.9 (99.6)
Redundancy	20.7 (21.3)	5.5 (5.1)	48.8 (38.3)	23.4 (23.5)
Refinement				
Resolution (Å)	85.6–3.2 (3.3–3.2) ^e	74.7–3.0 (3.1–3.0) ^e	68.4–2.6 (2.7–2.6) ^e	84.9–1.8 (1.9–1.8) ^e
No. reflections	17624 (1292)	20395 (1238)	17459 (1608)	51025 (3345)
<i>R</i> _{work} / <i>R</i> _{free} (%)	25.5 / 28.0	25.4 / 27.8	22.9 / 25.8	17.9 / 19.9
No. atoms				
Protein	7292	7241	3672	3775
Ions/monoolein/PEG	27	126	125	294
Water	0	0	0	156
<i>B</i> factors (Å ²)				
Protein	31.18	46.54	48.19	20.55
Ions/monoolein/PEG	32.77	45.10	58.48	48.24
Water	N/A	N/A	N/A	28.35
R.m.s. deviations				
Bond lengths (Å)	0.005	0.005	0.003	0.003
Bond angles (°)	1.02	0.67	0.62	0.66

^a Merged from 3 crystals.^b Merged from 2 crystals.^c Merged from 7 crystals (2 collected at wavelength of 0.98 Å and 5 at 1.65 Å).^d Merged from 6 crystals.^e Values in parentheses are for highest-resolution shell.

Supplementary Table 2. Comparison of mutagenesis data for MurJ_{TA} and MurJ_{EC}

Residues in TA	Residues in EC	MurJ _{TA}		MurJ _{EC}		Location
		Kuk et al., 2017, and this study	Butler et al., 2013, 2014	Zheng et al., 2018		
S17	S17	A		L W	P T A	TM1
R18	R18	A	A C E K	P	C S L G H	TM1
R24	R24	A	A C E K	G	L Q P	TM1
D25	D25	A N	C	H Y N	G V A E	TM1
R52	R52	A	A C E K	C	S L P H	TM2
E57	E57	A	C	K	Q A V G D	TM2
N162	N168	A		K*	I D H Y S T	TM5
Q229	Q244	A	C	L	E K P R H	TM7
N231	S246	A		C	A P T F Y	TM7
D235	N250	A N L	C	K	D Y H T I S	TM7
R255	R270	A	A C E K	P	C S L H	TM8
R352	K368	A Q	C	E I	Q T K N	TM10
N374	T394	A L		R K	P S A M	TM11
D378	N398	N L A			D H Y T S I K	TM11
T394	S413	C V A		Y	A P T F C	TM12

*Nucleotide 504 C to G and to A mutations, although resulting in synonymous N168K mutation, one led to a fold change of 13 and the other 2. In this table, we choose 13 for categorization.

Table Legend:

Kuk <i>et al.</i> , 2017 and this study,	Butler <i>et al.</i> , 2013 2014	Zheng <i>et al.</i> , 2018
No complementation	No complementation	Mutation frequency fold change >5
Partial complementation	Complementation but sensitive to low osmolarity	Mutation frequency fold change >2.5
Complementation	Complementation	Mutation frequency fold change <2.5

Supplementary Table 3. Sodium Fo – Fc omit peak heights and coordination distances

Structure	Na⁺ Fo – Fc omit peak height	Na⁺ coordination distance (in Ångstrom)				
		Asp235 OD1	Asn374 OD1	Asp378 OD1	Val390 O	Thr394 OG1
Inward closed	7 sigma	2.49	2.32	2.45	2.39	2.35
Inward occluded	9 sigma	2.44	2.43	2.40	2.40	2.41
Outward	19 sigma	2.45	2.26	2.42	2.33	2.33

Supplementary Table 4. List of primers used in this study

Primer name	Sequence (5' to 3')
Sodium site	
MurJ_D235L_F	agccagatcaaacactgtggtgctaataaacgtggtttctttctac
MurJ_D235L_R	gtagaaagaaccacgttcattagcaccacagtggtgatctggct
MurJ_D235N_F	cagatcaaacactgtggtgaacatgaacgtggtttctt
MurJ_D235N_R	aagaaccacgttcattggtcaccacagtggtgatctg
MurJ_D378A_F	gcctgagcaatatcattctggctattatctttggcctgaaata
MurJ_D378A_R	tatttcaggccaaagataatagccagaatgatattgctcaggc
MurJ_D378L_F	gtagcctgagcaatatcattctgctaattatctttggcctgaaatacggc
MurJ_D378L_R	gccgtatttcaggccaaagataatagcagaatgatattgctcaggctaac
MurJ_D378N_F	ttagcctgagcaatatcattctgaatattatctttggcctgaaatac
MurJ_D378N_R	gtatttcaggccaaagataatattcagaatgatattgctcaggctaa
MurJ_N374L_F	cgcgaccattgtagcctgagcctaatacattctggatattatctttgg
MurJ_N374L_R	ccaaagataatccagaatgattaggctcaggctaacaatggctcgcg
MurJ_T394A_F	gttgcgctggcggccagcattgcgg
MurJ_T394A_R	ccgcaatgctggccgcccagcgcgaac
MurJ_T394C_F	cgttgcgctggcgtgcagcattgcgggc
MurJ_T394C_R	gcccgcaatgctgcacgcccagcgcgaacg
MurJ_T394V_F	cgttgcgctggcggtcagcattgcgggc
MurJ_T394V_R	gcccgcaatgctgaccgcccagcgcgaacg
Other mutagenesis	
MurJ_D25A_F	cctgggtctgttctgctgtactgttcgcaaaat
MurJ_D25A_R	atthtgcgaacagtagacagcagcaaacagaccagg
MurJ_D25N_F	gtatcctgggtctgttctgtaatgtactgttcgcaaaatac
MurJ_D25N_R	gtattttgcgaacagtagcattacgaacagaccaggatac
MurJ_R352A_F	gcatctatagcaccattagcgtatgctatcatgccatcaaaa
MurJ_R352A_R	ttttgatggcatgatagctagcgttaattggtgctatagatgc
MurJ_R352Q_F	ggcatctatagcaccattagccagagctatcatgccatcaaaaata
MurJ_R352Q_R	tattttgatggcatgatagctctggctaattggtgctatagatgcc
Cysteine accessibility	
MurJ_A29C_F	gtctgtttcgtgatgtactgttctgtaaatacttcggtgtctcttacga
MurJ_A29C_R	tcgtaagagacaccgaagtatttacagaacagtagacacacgaacagac
MurJ_I247C_F	ctttctacgacaaaggttctgctcttatctgcaatacgcgt
MurJ_I247C_R	acgcgtattgcagataagagcaggaacctttgctgtagaaag
MurJ_S113C_F	cctgttcggtgctggtgttctcatgaaactaag
MurJ_S113C_R	cttagttcatgagaacaaccagcaccgaacagg
MurJ_S61C_F	cggtaggggtgcaatgtgttctgcattgtacctc
MurJ_S61C_R	gaggtacaatgcagaacacattgcaccctcaccg
MurJ_S69C_F	ctgcattgtacctctgtactgtgaaaaatccggtg
MurJ_S69C_R	caccggattttcacagtagaggtacaaatgcag
MurJ_S161C_F	ggctctgactccgtctatctgtaacattaccatcattattg
MurJ_S161C_R	caataatgatggtaattgttacagatagacggagtcagagcc

MurJ_S240C_F	gtggacatgaacgtggtttgtttctacgacaaaggttc
MurJ_S240C_R	gaacctttgtcgtagaacaaaccacgttcatgtccac
MurJ_S248C_F	cgacaaaggttccatctgttatctgcaatacgcgt
MurJ_S248C_R	acgcgtattgcagataacagatggaacctttgtcg
MurJ_S254C_F	tcttatctgcaatacgcgtgccgtttctacctgc
MurJ_S254C_R	gcaggtagaacggcacgcgtattgcagataaga
MurJ_S274C_F	tatccactgttctgtgcaaatctccaacgatcg
MurJ_S274C_R	cgatcgtggagattttgcacagaacaacagtgata
MurJ_S277C_F	ctgtgttctgtccaaaatctgcaacgatcgtaaaaactcaa
MurJ_S277C_R	ttgaagttttacgatcgttgcagattttggacagaacaacag
MurJ_T232C_F	tggtcagccagatcaactgtgtgggtggacatgaacg
MurJ_T232C_R	cgttcatgtccaccacacagttgatctggctgacca
MurJ_T270C_F	ctgtttgctgtatccgtatcctgtgttctgtccaaaatctc
MurJ_T270C_R	gagattttggacagaacaacacaggatcggatacagcaaacag
MurJ_V34C_F	gttcgcaaaatactcggttgctcttacgagctggatgca
MurJ_V34C_R	tgcattccagctcgttaagagcaaccgaagtattttgcgaac